

# BiPMAP: A Toolbox for Predictions of Perceived Motion Artifacts on Modern Displays

Guanghan Meng\*, Dekel Galor\*, Laura Waller, and Martin S. Banks

**Abstract**—Presenting dynamic scenes without incurring motion artifacts visible to observers requires sustained effort from the display industry. A tool that predicts motion artifacts and simulates artifact elimination through optimizing the display configuration is highly desired to guide the design and manufacture of modern displays. Despite the popular demands, there is no such tool available in the market. In this study, we deliver an interactive toolkit, Binocular Perceived Motion Artifact Predictor (BiPMAP), as an executable file with GPU acceleration. BiPMAP accounts for an extensive collection of user-defined parameters and directly visualizes a variety of motion artifacts by presenting the perceived continuous and sampled moving stimuli side-by-side. For accurate artifact predictions, BiPMAP utilizes a novel model of the human contrast sensitivity function to effectively imitate the frequency modulation of the human visual system. In addition, BiPMAP is capable of deriving various in-plane motion artifacts for 2D displays and depth distortion in 3D stereoscopic displays.

## I. INTRODUCTION

MODERN displays constitute an interface bridging the two ends of an information delivery system: the electronic signal supplied to the display, and the human observers receiving the information converted to light by the interface. For effective communication and pleasant visual experiences, the interface needs to be optimized to fit the capabilities of human visual systems. Therefore, display manufacturers have made tremendous efforts to optimize the design of their display products, e.g., monitors, projectors, virtual-reality (VR) and augmented reality (AR) headsets, towards achieving the appropriate representation of dynamic scenes. Although the motion of an object is always presented through a discrete sequence of static views, a proper design of the display device will ensure human observers see the object moving smoothly across the display [1].

A variety of motion artifacts must be considered when designing a display device for presentation of dynamic scenes, e.g., flicker, judder, edge banding, motion blur, color breakup, and depth distortion. Flicker, a perceived discontinuity in frame brightness, can be eliminated with a frame rate beyond 60-75 frames per second (FPS), which has been widely adopted in television and cinema for many years [2]. However, other artifacts tend to persist in dynamic scenes with high-speed movements [3]–[6]. In addition, other factors such as the

luminance [7] and viewing distance, can significantly affect the perception of displayed motion. Consequently, a tool capable of thorough and accurate predictions of all the above motion artifacts perceived by human observers given an arbitrary set of user-defined parameters is highly desired to guide the design of modern displays.

To accurately simulate the perceived motion artifacts, one needs to reproduce the information processing exerted on an input stimulus by the human visual system. The contrast sensitivity function (CSF), a cornerstone of many mathematical models in vision science, defines the response of the human visual system to luminance variation in both space and time by identifying the inverse of the minimum contrast visible at distinct spatiotemporal frequencies. Therefore, the CSF model enables the analysis of visual perception in the frequency domain. Accordingly, the window of visibility, an important concept proposed by Andrew Watson in 1986 [1], defines the frequency bands as transmissive, thus visible, to the human visual system by outlining the boundary of the domain corresponding to the non-zero section of the CSF. On that account, as long as the displayed motion has a frequency spectrum identical to that of the continuous trajectory from which the displayed stimulus is sampled inside the window of visibility, the motion presented on the display will appear smooth to observers without undesirable artifacts [1]. Furthermore, since luminance alters the shape of CSF conspicuously, an ideal CSF model should encompass luminance, spatial and temporal frequencies across the entire window of visibility while remaining computationally simple for practical use.

In this study, for the first time to our knowledge, we developed a ‘click-and run’ toolbox to guide the design and manufacturing of modern displays, named Binocular Perceived Motion Artifact Predictor (BiPMAP), for prediction and visualization of perceived motion artifacts. Considering computation speed and simplicity, the visual stimulus processed through BiPMAP is configured as the contrast distribution across the 1D trajectory of a bright object moving at a constant speed along a horizontal line over a dark background. Our main contributions are summarized as follows:

- 1) We created a pipeline that visualize a variety of predicted motion artifacts through analysis in the Fourier domain, making use of the window of visibility concept.
- 2) We proposed a simple CSF model accounting for the three major dimensions: spatial frequency, temporal frequency and luminance covering the entire window of visibility for accurate motion artifact prediction.
- 3) We designed a user interface that takes a comprehensive list of user-defined display and viewing parameters, and

\*Guanghan Meng and Dekel Galor contributed equally to the work.

All authors are with University of California, Berkeley

Guanghan Meng: guanghan\_meng@berkeley.edu

Dekel Galor: galor@berkeley.edu

Laura Waller: waller@berkeley.edu

Martin S. Banks: martybanks@berkeley.edu

delivered the toolbox as an interactive executable file.

- 4) For the first time, we quantified the perceived disparity, i.e., depth distortion in sequential-field stereo displays under the concurrence of eye motion.

## II. BACKGROUND AND RELATED WORK

### A. Time-sampled representation of a moving stimulus

A displayed visual stimulus is a time-sampled version of the corresponding real continuous motion. A useful method for representing and analyzing a sampled motion was proposed by Watson et al. in 1986 [1], which is briefly reviewed below and adapted for our toolkit. If we consider a vertical line infinitely long with unit contrast moving horizontally, the contrast distribution along the motion axis (horizontal in this case) of the moving stimulus is:

$$l(x, t) = \delta(x - rt) \quad (1)$$

where  $l(x, t)$  specifies the contrast as a function horizontal position  $x$  and time  $t$ . The sampled stroboscopic stimulus presented on a display, ergo, is represented by the multiplication of the continuous contrast distribution and a sampling function:

$$l_s(x, t) = \Delta t \delta(x - rt) \sum_{n=-\infty}^{\infty} \delta(t - n\Delta t) \quad (2)$$

$\Delta t$  is to equalize the integral contrast within each sampling cycle between the continuous and sampled spaces.

If the sampled stimulus is not stroboscopic and the pixel on the display is illuminated for a finite proportion of each frame interval, i.e., sample and hold, the stimulus now has a staircase presentation which becomes:

$$l_z(x, t) = (\Delta t \delta(x - rt)) \sum_{n=-\infty}^{\infty} \delta(t - n\Delta t) * z(x, t) \quad (3)$$

where  $z(x, t)$  is unit staircase function:

$$z(x, t) = \omega_s \delta(x) \text{rect}(t\omega_s) \quad (4)$$

and  $\omega_s = 1/\Delta t$  is the sampling frequency.

To analyze motion artifacts perceived by human observers, we will approach this problem in the frequency domain. First, the frequency spectra of the continuous stimulus:

$$L(u, \omega) = FT_{x,t}[l(x, t)] = \delta(ru + \omega) \quad (5)$$

Where  $u$  is the spatial frequency, and  $\omega$  is the temporal frequency. The above frequency spectrum is a line with an infinite length and a slope equal to the opposite reverse of the motion velocity in the space-time domain. In contrast, the stroboscopic sampled stimulus gives rise to a frequency spectrum of:

$$L_s(u, \omega) = FT_{x,t}[l_s(x, t)] = \sum_{n=-\infty}^{\infty} \delta(ru + \omega - n\omega_s) \quad (6)$$

Which contains infinite number of replicas of the frequency spectrum of the continuous motion, with a spacing of  $\omega_s$  among intersects on the temporal frequency axis. At last, for

the staircase representation of a sampled stimulus, a temporal *sinc* modulation is applied to each replica, given by:

$$L_z(u, \omega) = \left[ \sum_{n=-\infty}^{\infty} \delta(ru + \omega - n\omega_s) \right] \text{sinc}\left(\frac{\omega}{\omega_s}\right) \quad (7)$$

### B. Contrast sensitivity function (CSF) and window of visibility

Contrast sensitivity is defined as the inverse of the minimum contrast enabling human visual system to detect light variations in space and time at a given frequency. The CSF, therefore, encapsulates the contrast sensitivity values across different frequencies, which has limited extents in both dimensions, i.e., spatial frequency and temporal frequency, due to the limited spatiotemporal resolution of human eyes. The concept of window of visibility was first proposed by Andrew Watson in 1986 [1], defining a rectangular window in the frequency space that encloses all the frequency components visible to human eyes. As a result, although the displayed stimulus is always a sequence of discrete static views, as long it is indistinguishable from its corresponding continuous motion for the domain inside the window of visibility, the sampled representation will appear smooth and continuous to viewers. More specifically, provided that there is only one replica from the frequency spectrum of the sampled stimulus enclosed by the window of visibility, the sampled representation on display will be perceived as equivalent to the original smooth motion. Despite the robustness of frequency-domain analysis enabled by the concept of window of visibility, a binary rectangular window ignoring the shape and amplitude of the CSF is clearly an oversimplification of the frequency response of the human visual systems. Furthermore, other factors including luminance alters the shape of CSF significantly. Accordingly, an upgraded CSF model, named pyramid of visibility was proposed in 2016 [7] where the low-frequency region is omitted and the high-frequency bands are fit with linear models (in log space), with the temporal and spatial frequencies considered independent and separable. The pyramid of visibility defines the CSF as the 3D surface, which has a height that grows with luminance. Additional factors also modulate the CSF, e.g., field of view, eccentricity, and object size [8]–[10].

### C. Motion artifacts on a 2D display

There are a variety of motion artifacts we are concerned about:

1) *Flicker*: Flicker describes a perceived temporal discontinuity in the illumination from the display. In the space-time domain, it is presented as non-uniform light intensity of the perceived motion along the time axis. In the frequency domain, flicker will be perceived when replicas encroach the window near a spatial frequency of zero, i.e., when the replicas intersect with the temporal frequency axis inside the window of visibility and the replicas has non-zero amplitude near the intersections [3]. Sample-and-hold, i.e., staircase representations of a sampled stimulus, applies a *sinc* attenuation to its frequency spectrum with the first minimum at the sampling frequency  $\omega_s$  on the temporal axis, thus effectively suppresses flicker.

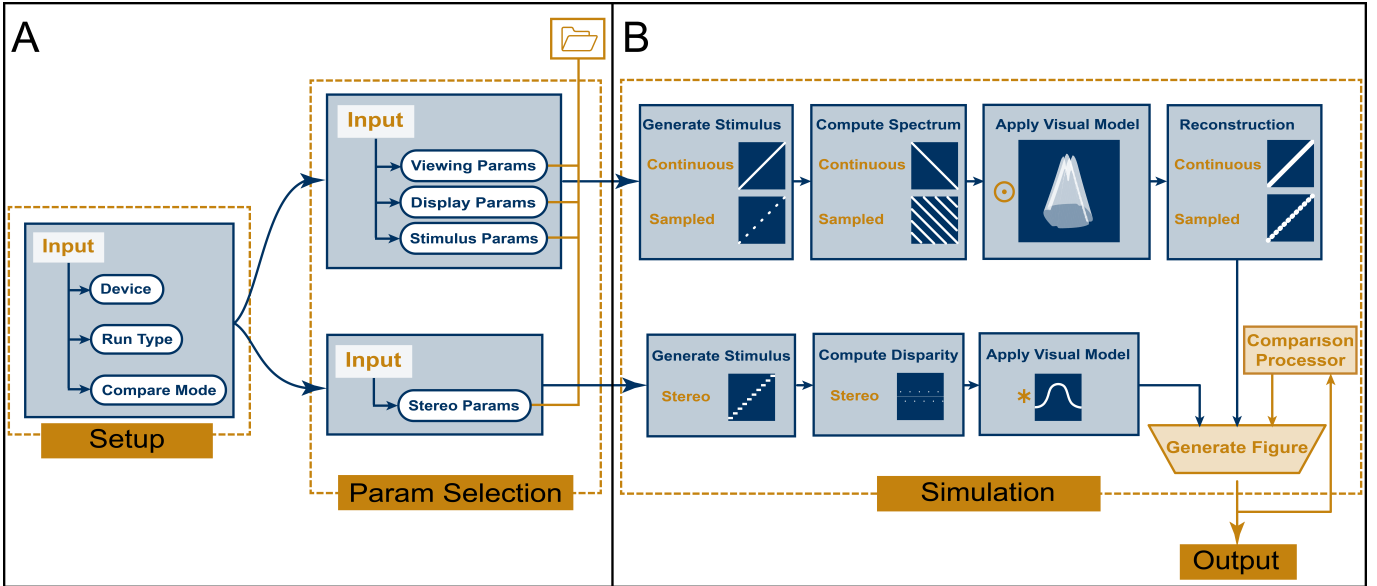


Fig. 1. Overview of BiPMAP. (A) Front-end with all user-defined parameters, divided into two components: Setup (configuration inputs) and Parameter Selection (simulation variables). (B) Back-end pipeline for artifact predictions, containing two individual streamlines—2D (top) and Stereo (bottom)—and a figure generation step. When “Compare Mode” in the Setup component of (A) is enabled, the Comparison Processor integrates information from past runs and outputs a comparison figure.

2) *Judder*: Judder, an artifact depicting unsmooth perceived motion, occurs when the window of visibility encapsulates more than one replicas of the frequency spectrum of the continuous motion.

3) *Edge banding*: Edge banding commonly occurs together with judder, and describes an artifact containing multiple ghost images of an edge from the displayed object. The visibility of edge banding increases for displays employing a multi-flash protocol, i.e., with repeated presentations of each frame [5].

4) *Motion blur*: Motion blur refers to the phenomenon when a sharp edge is perceived as thicker and blurrier [4]. When a viewer is smoothly tracking a displayed moving object with their eyes, the perceived image remains stationary with respect to the retina. This effectively suppresses artifacts like judder, although it can incite motion blur when the duration of illumination for each frame is high.

5) *Color breakup*: Color breakup, known as the rainbow effect, is an artifact observed on displays presenting colors sequentially [11]. With color breakup, a single chromatic color is perceived as distinct fringes or blocks of red, green and blue illumination. Color breakup tends to become more evident when viewers are tracking the moving stimulus being displayed, and can be corrected via multiple categories of strategies [12]–[14], including applying spatial offsets to the 2<sup>nd</sup> and 3<sup>rd</sup> colors being presented [15].

#### D. Depth distortion stereoscopic displays

Besides all the motion artifacts described above, 3D displays have another dimension where artifact can occur: depth distortion. Stereoscopic displays constitute the most common type of 3D displays, where the 3D experience is based on “depth cues”, i.e., properties of the retinal images that signify variations in depth [16]. Binocular disparity, the spatial differences in the images seen by the two eyes, is the main depth cue

utilized in stereoscopic displays. Temporal interlacing protocol is a common strategy for stereoscopic displays [3] with an overlapping path for binocular vision, where the same display is shared between the left and right eyes but only one of the eyes receives light at a given time. Such a temporal delay between inputs to each eye causes a moving object to appear displaced in depth, i.e., depth distortion, as a result of non-zero binocular disparities [3], [17], [18].

### III. OVERALL DESIGN OF BIPMAP

We have the following specific design goals for the BiPMAP toolkit:

- 1) The toolkit should account for a comprehensive list of user inputs, including the velocity of the moving stimulus, and all common display and viewing parameters.
- 2) The toolkit should adopt an effective and simple CSF model for accurate prediction of perceived motion artifacts.
- 3) The toolkit should present continuous and sampled stimulus side-by-side, so that any motion artifacts exclusively visible in the perceived sampled stimulus can be easily identified and eliminated by adjusting design parameters.
- 4) The toolkit should visualize a variety of motion artifacts, including both in-plane artifacts and depth distortion.

BiPMAP consists of an interactive user interface (Fig. 1 A and Fig. 2), and a computational pipeline (Fig. 1 B).

#### A. General inputs and available running modes of BiPMAP

1) *Device selection*: BiPMAP automatically detects available computation devices in the machine and lists them under the device selection button (Fig. 11A, Fig. 2 D, which allows users to select the preferred device for the processing.

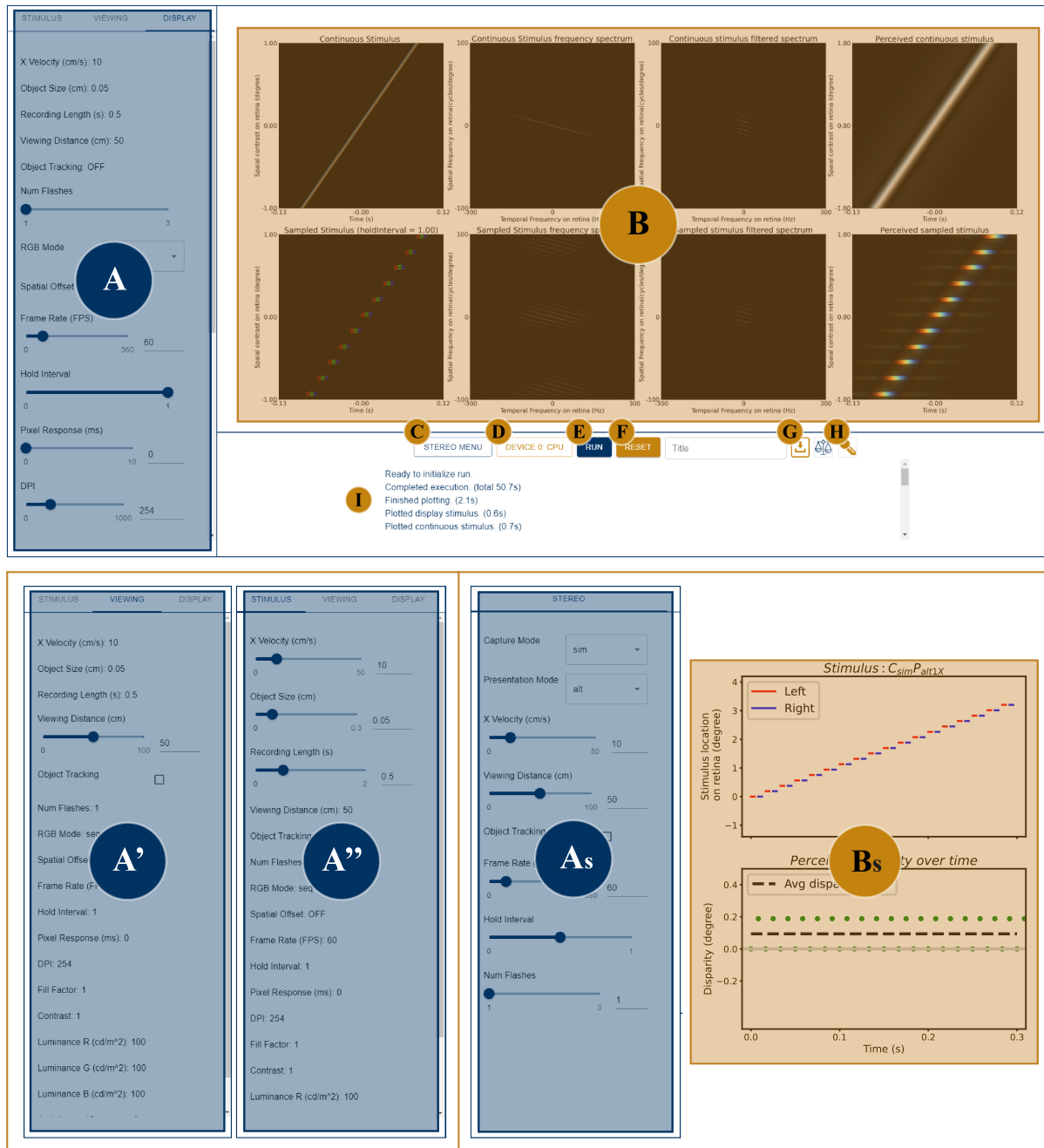


Fig. 2. The view of BiPMAP User interface (UI). (A - As) Parameter Selection. (B - Bs) Output section. (C - H) Setup section. (As) (Bs) User-accessible parameters and example output, respectively, under the stereoscopic mode. (A) (A') (A'') Parameters accessible under the "display", "viewing" and "stimulus" tabs, respectively, under the default 2D display mode. (B) Example output for in-plane artifact predictions. (C) The toggle button to switch between planar artifacts and depth distortion calculations. (D) To expand a list of available devices and their memory for user to choose from. (E) To initiate the run with given parameters. (F) To reset the parameters to their default values and empty all memory. (G) To download the figure in display and save under the specified name. (H) Toggle buttons for the "compare mode"

2) *Run type*: There are two different running modes of BiPMAP: planar motion artifact predictions and binocular disparity calculations in temporally-interlacing stereoscopic displays. Users can switch between the two modes using the toggle button in Fig. 2C. The default mode is to predict in-plane artifacts on a 2D display, while the 'stereo menu' will output graphs of disparity values.

3) *Compare Mode*: To address the needs from our users who want to compare results from runs side by side, BiPMAP

can run under 'compare mode' by checking the the option with a scale' icon (Fig. 2H, left). The 'key' icon next to the 'scale' is for users to choose the 'master' run by clicking the button after the round of processing that will be set as the reference during the comparison. By default, i.e., without a selection of master run, the perceived continuous motion will be chosen as the reference.

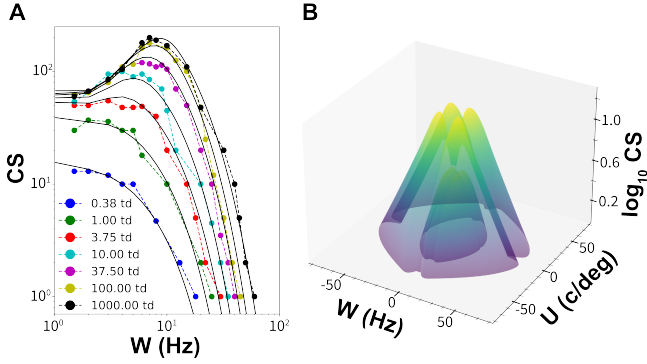


Fig. 3. A novel model of the contrast sensitivity function (CSF) of the human visual system. (A) The empirical temporal CSF model (solid lines) obtained from fitting experimental data (round markers). (B) The dependence of the spatiotemporal CSF on luminance, plotted at values of  $0.5cd/m^2$  (inner cone) and  $160cd/m^2$  (outer cone).

### B. Pipeline for predictions of planar motion artifact

Our pipeline consists of the following four steps to compute and visualize in-plane/horizontal perceived motion artifacts, as presented in Fig. 1:

- Configure the continuous and sampled motion with user-defined parameters.
- Compute the discrete Fourier transforms (DFT) of the continuous and sampled stimuli.
- Apply the spatiotemporal filtering effect of human CSF, i.e., a non-binary window of visibility to obtain the perceived spectra.
- Reconstruct the perceived stimuli using the inverse DFT, with continuous and sampled representations side-by-side, so that any motion artifacts can be easily identified from the sampled motion.

1) *Input parameters and configuration of stimulus*: There are three sets of input parameters to fully define the visual stimulus: Stimulus properties (Fig. 2 A''), display parameters (Fig. 2 A'), and viewing parameters (Fig. 2 A).

**Display parameters** in Fig. 2 A:

- **Num Flashes (number of flashes)**: This parameter indicates the number of times each frame is presented on the screen.
- **RGB Mode**: three options are available for this parameter: black and white (BW), sequential field RGB (RGB-seq), and simultaneous RGB presentation (RGB-simul). If the user is not concerned about color artifacts, black and white mode is recommended for the benefit of processing speed and memory consumption.
- **Frame Rate**: frames per second (FPS), equal to the number of samples along the motion trajectory each second, and is different from presentation rate when the number of flashes is larger than 1 or when RGB mode is sequential.
- **Hold Interval**: the proportion of the frame interval during which the pixel is illuminated, ranges from 0 to 1 (0 for a stroboscopic display).
- **Pixel Response**: the time it takes for a pixel to light up or dim out. The hold interval above is defined as the

start of the rising course to the end of the falling course of the pixel luminance. The rising and falling courses are both modeled as linear processes for simplicity of computation.

- **DPI**: dots or pixels per inch. Pixel size will be calculated as  $1/DPI$ .
- **Fill factor**: pixel fill factor, a value from 0 to 1, determines the gap between pixels. Default value: 1.
- **Contrast**: the contrast of the moving object, defined as:

$$contrast = \frac{L_{max} - L_{min}}{L_{max} + L_{min}} \quad (8)$$

$L$  is luminance here.

- **Luminance R/G/B**: the luminance of stimulus for the three colors. Background brightness will be calculated using equation (8).

**Viewing parameters** in Fig. 2 A':

- **Viewing distance**: the distance from the display to the viewer's eyes.
- **Object tracking**: a checkbox to decide whether viewer's eyes will track the moving stimulus. If checked,  $v_{eye} = v_{stimulus}$  and the on-retina velocity of the stimulus becomes 0.

**Stimulus Parameters** in 2A'':

- **X Velocity**: the input is in cm/s, and will be converted to degrees/s within the pipeline using the user-defined viewing distance.
- **Object Size**: the input is in cm, and will be converted to the number of pixels and degrees using pixel size and viewing distances defined above.
- **Recording Length**: in seconds, decides the total duration of the sampling. Longer recording length improves spectral resolution but is more demanding in computation speed and is also bounded by the memory of the processing device. The default recording length is  $0.5s$ , which can be adjusted according to memory capacity and computational power of the GPU/CPU. When using the toolbox in RGB mode and the computational device is a GPU with  $<24GB$  of dedicated memory, it is recommended to decrease the recording length.

2) *A novel three-dimensional CSF model*: For reliable artifact predictions, a non-binary CSF is applied to the frequency spectra of input stimuli. We proposed a robust novel CSF model over existing models, e.g., pyramid of visibility which is only valid for high-frequency bands [7], or the stelaCSF model that is thorough but complicated with five dimensions [8]. We devoted our attention to the three main dimensions: spatial frequency, temporal frequency, and luminance. Considering that the CSF is nearly separable at high frequency ranges, we opted for computation simplicity and extended the separability assumption to the entire spatial and temporal Fourier domain, deriving our CSF model as:

$$CS(u, \omega) = \sqrt{CS_s(u)CS_t(\omega)} \quad (9)$$

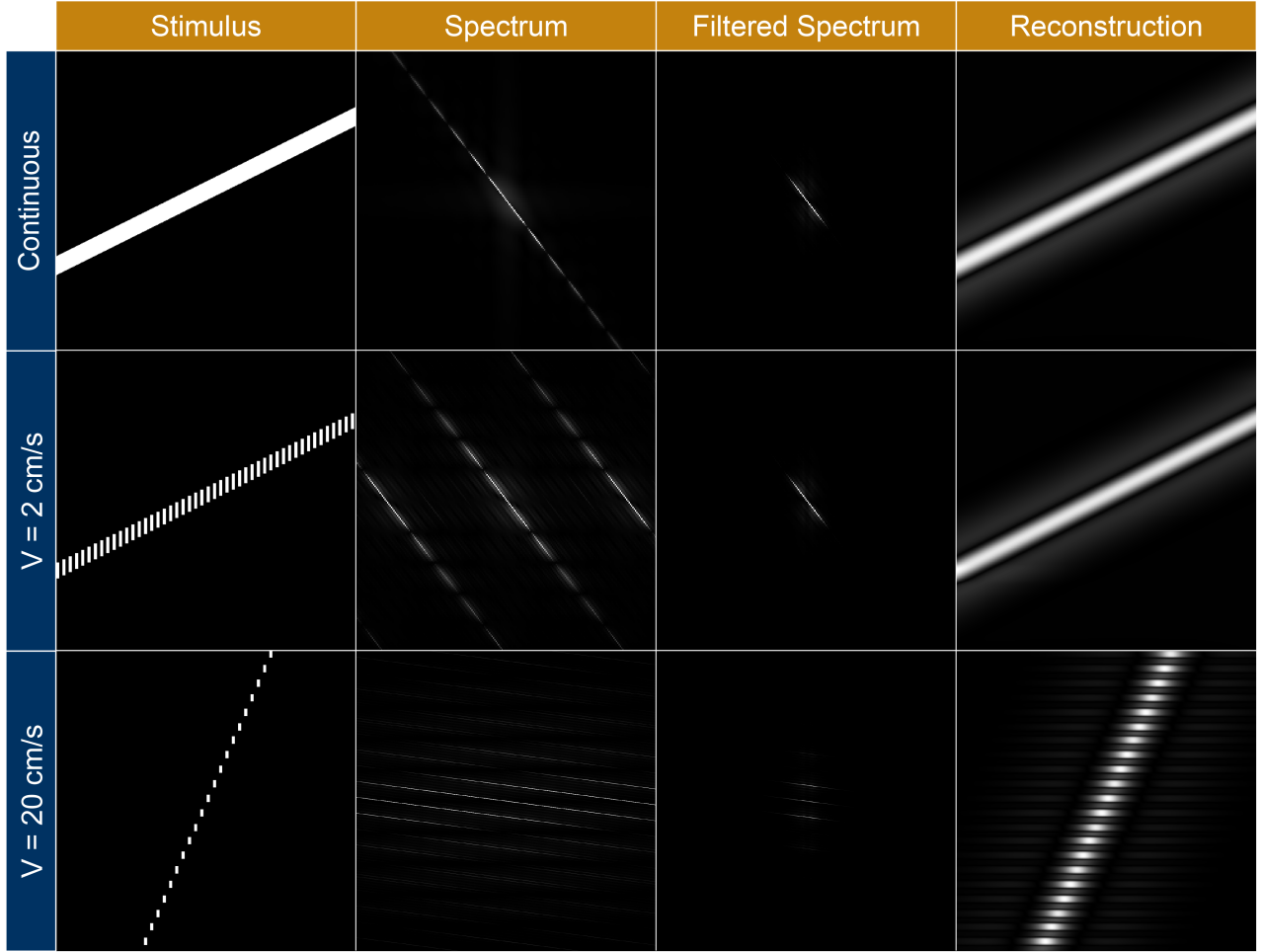


Fig. 4. The effect of velocity on judder. 'Stimulus' column: the configured stimulus with user-defined parameters. 'Spectrum' column: the 2D discrete Fourier transform (DFT) of the stimulus. 'Filtered Spectrum' column: the spectrum filtered by the CSF. 'Reconstruction' column: the perceived stimulus reconstructed using the inverse DFT of the filtered spectrum. Top two rows: results of continuous (top row) and sampled stimulus (middle row) with a motion velocity of  $2\text{cm/s}$ . No motion artifacts perceived from the sampled stimulus. Bottom row: results of a sampled stimulus with a motion velocity of  $20\text{cm/s}$ , with obvious discontinuity (judder) in the perceived image. Pixel density:  $300\text{dpi}$ . Frame rate:  $240\text{fps}$ . Holder interval:  $0.5$

Where  $CS_s(u)$  is the spatial CSF,  $CS_t(\omega)$  is the temporal CSF. We used an existing spatial CSF model [10]:

$$CS_s(u) = \frac{5200e^{-0.0016u^2(1+100/L)^{0.08}}}{\sqrt{\left(1 + \frac{144}{X_o^2} + 0.64u^2\right)\left(\frac{63}{L^{0.83}} + \frac{1}{1-e^{-0.02u^2}}\right)}} \quad (10)$$

Where  $X_o$  is the angular object size,  $L$  is luminance,  $u$  is the spatial frequency. Since there is no robust temporal CSF model that incorporates luminance, we fit an empirical temporal CSF to a set of published psychophysical data [19], [20] (Fig. 3A):

$$CS_t(\omega) = \frac{5360L^{2.51}e^{-0.16\omega L^{-0.017}}}{\sqrt{\left(\frac{a\omega^b L}{L^{-4.98}} + 1\right)\left(\frac{c}{L} + \frac{d}{1.007 - e^{f\omega^{3.8}}}\right) - L^5}} \quad (11)$$

where  $a = 2.1e + 9$ ,  $b = 9e - 4$ ,  $c = 1.2e - 7$  and  $d = -2.7e - 4$ . Since the data was in terms of retinal illuminance rather than luminance, we utilized a conversion formula from the previously published spatial CSF model [10].

Based on equations (9) - (11), we obtained a spatiotemporal CSF model accounting for all three major dimensions, and the height, i.e., the peak contrast sensitivity, grows with

increasing luminance as expected. For example, the peak CS rises by a factor of 4 as luminance increases from  $0.5\text{cd/m}^2$  to  $160\text{cd/m}^2$  (Fig. 3B).

### C. Assessment of depth distortion in stereoscopic displays

Under the stereoscopic mode, only the parameters involved in disparity calculations will be accessible to the user. Fig.  $2A_s$ ,  $B_s$  manifests the user inputs and an example output from disparity calculation. **Parameters exclusive to binocular disparity calculation** in Fig.  $2A_s$ :

- **Capture mode:** simultaneous or alternating capture of scenes. Alternating capture is generally difficult to realize due to strict requirement for capture-display synchronization. Therefore, simultaneous capturing is the dominant capture mode and the default option here.
- **Presentation mode:** simultaneous or alternating presentation of the captured scenes. Simultaneous presentation is only feasible when each eye has access to an individual screen. Alternating presentation is the protocol for temporally-interlacing stereoscopic display, where the

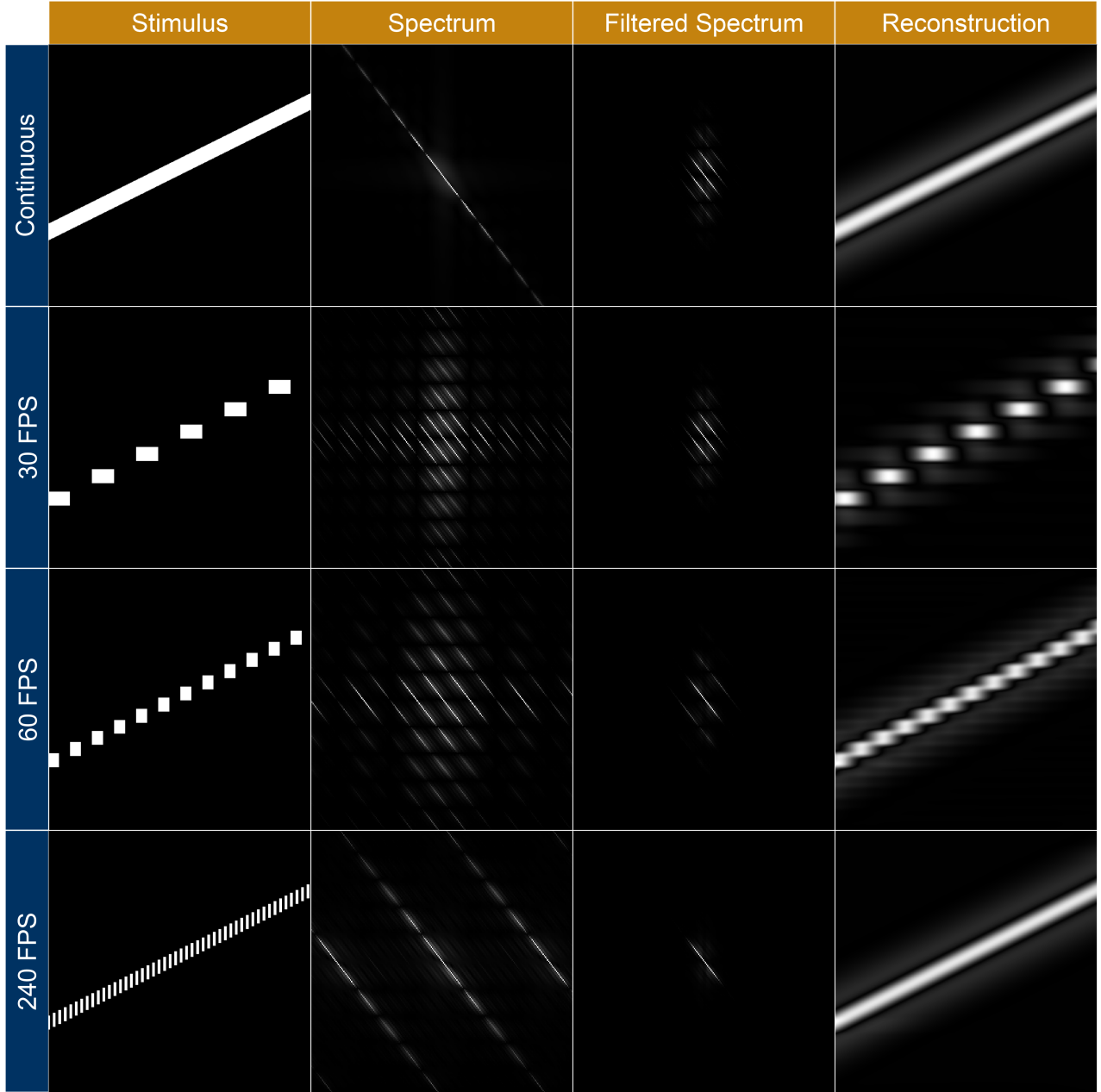


Fig. 5. The effect of frame rate on judder. 'Stimulus' to 'Reconstruction' columns arranged in the same way as in Figure 4. Top row: results from the continuous stimulus.  $2^{nd}$  from the top row: Output from a sampled stimulus at  $30fps$  sampling rate, with flicker and judder.  $2^{nd}$  from the bottom row: residual judder but no flicker at a frame rate of  $60fps$ . Bottom row: smooth motion perceived at a frame rate of  $240fps$ . Motion velocity:  $2cm/s$ . Pixel density:  $300dpi$ . Frame rate:  $240fps$ . Holder interval: 0.5

captured scene is presented to only one eye at a given time.

#### IV. TASK-BASED FUNCTIONALITY OF BIPMAP

##### A. The effect of stimulus velocity and frame rate on flicker and judder

Based on equations (1) - (7), incremental velocity leads to counterclockwise rotation in the space-time domain and the frequency domain. As demonstrated in Fig. 4, when velocity grows from  $2cm/s$  to  $20cm/s$ , clear counterclockwise rotations are observed from the original stimuli (Fig. 4, left column), the frequency spectra (Fig. 4, second from the left

column), the spectra filtered with CSF (Fig. 4, second from the right column), and the perceived stimuli (Fig. 4, right column).

When  $v = 2cm/s$ , at a frame rate of  $240FPS$ , only 1 replica of the frequency spectrum from the continuous stimulus is transmitted through the CSF (Fig. 4, middle row, filtered spectrum), i.e., the frequency spectra of the continuous and sampled representation of the motion remain identical inside the window of visibility (Fig. 4, top and middle rows, filtered spectrum), they are perceived as the same smooth motion by observers (Fig. 4, top and middle rows, Reconstruction). In contrast, when  $v = 20cm/s$ , more than 3 replicas in the frequency spectrum of the sampled motion fit within the

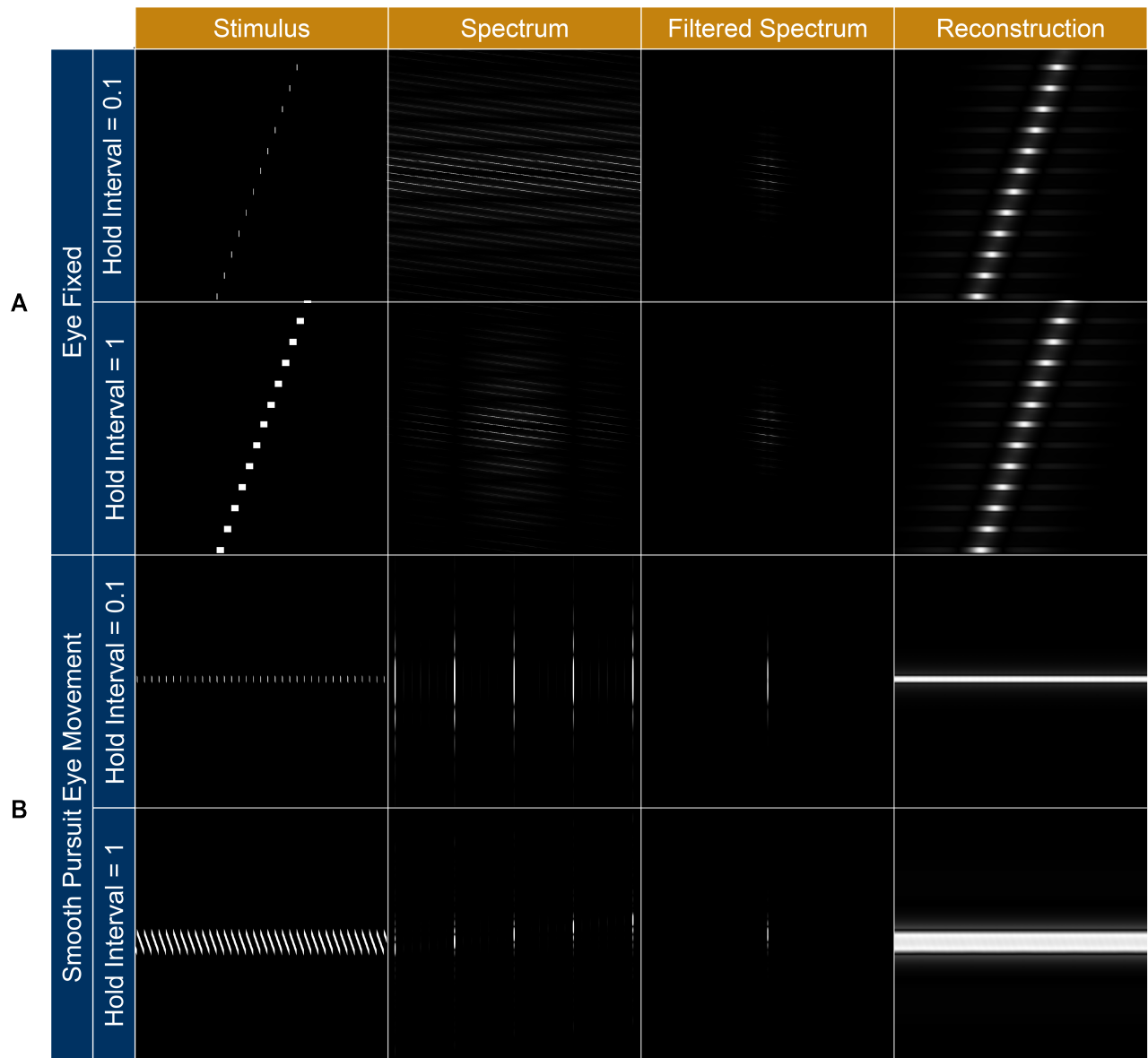


Fig. 6. The effects of hold interval and object tracking on motion blur. 'Stimulus' to 'Reconstruction' columns arranged in the same way as in Figure 4 and Figure 5. (A) An increase from 0.1 to 1 of Hold interval does not noticeably affect motion artifacts when the eye is fixed. (B) With eye motion, a larger hold interval significantly exacerbates the motion blur. Stimulus motion velocity on display:  $20\text{cm/s}$ . Pixel density:  $300\text{dpi}$ . Frame rate:  $140\text{fps}$ .

window of visibility. As a result, the reconstructed stimulus have visible gaps among samples, indicating a perceived discontinuous motion trajectory, i.e., judder. Note that the filtered spectrum (when  $v = 20\text{cm/s}$ ) only intersects with the temporal frequency axis once at the origin, thus each discrete segments in the perceived stimulus has overlaps with its neighbors along the time axis. Therefore, there is no visible flicker in this example, despite the persistence of judder artifact. The obstinacy of judder compared to flicker is also revealed in Fig. 5. In this set of examples,  $v = 4\text{cm/s}$  is maintained while the frame rate increases from 30 FPS (Fig. 5, second row) to 240 FPS (Fig. 5, bottom row). A larger frame rate, i.e., sampling rate, separates replicas in the sampled frequency spectra further apart, until only 1 remains inside the window of visibility and the perceived sampled representation (Fig. 5, bottom row) resembles the continuous ground truth

(Fig. 5, top row). Although flicker has been successfully suppressed at 60 FPS, the perceived motion remains clearly segmented, indicating the judder artifact.

#### B. Motion blur as a result of object tracking

When the visual stimulus contains a high speed motion, e.g.,  $20\text{cm/s}$ , as in Fig. 6, a frame rate of 100 FPS is not sufficient to suppress judder (Fig. 6, top 2 rows, 'Reconstruction' panel). Increasing the hold interval from 0.1 (Fig. 6, top row) to 1 (Fig. 6, second from the top row), applied a *sinc* attenuation to the frequency spectrum (Fig. 6, top two rows, 'Spectrum' panel), although the attenuation effect does not invade the window of visibility (Fig. 6, top two rows, 'Filtered Spectrum' panel). As a result, the hold interval does not impact the perceived judder artifacts. However, once

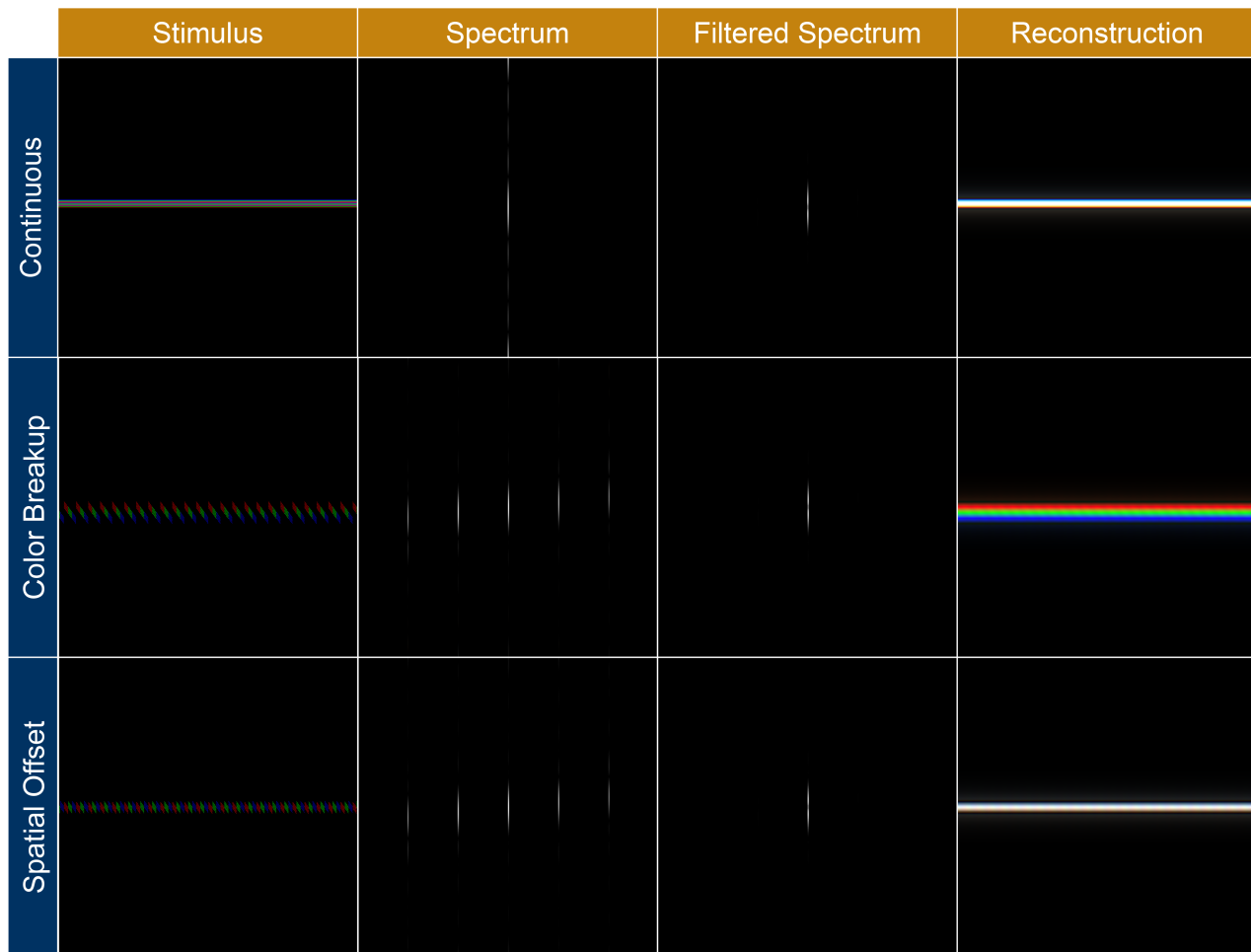


Fig. 7. The occurrence of color breakup in field-sequential color displays with eye motion. 'Stimulus' to 'Reconstruction' columns arranged in the same way as in Figure 4 through Figure 6. Top row: a continuous stimulus with R-G-B stripes indistinguishable in the perceived stimulus. Middle row: Sampled stimulus, with color breakup effect clearly visible. Bottom row: Sampled stimulus with spatial offsets to correct the color breakup. Stimulus motion velocity (on display):  $10\text{cm/s}$ . Pixel density:  $300\text{dpi}$ . Frame rate:  $100\text{fps}$ . RGB mode: *seq*. Hold interval: 1.

viewers track the moving stimulus being displayed (Fig. 6, bottom two rows), hold interval becomes a crucial parameter. When hold interval is 0.1, the object tracking, or smooth pursuit eye movement, enforces the retinal velocity of the stimulus to 0, so that the judder artifact completely vanishes. When hold interval increases to 1, however, another type of artifact, motion blur, becomes dominant (Fig. 6, bottom row). The blurred image perceived by viewers (Fig. 6, bottom row, 'Reconstruction' panel) results from the stacked diagonal line segments aligned along the horizontal motion trajectory (Fig. 6, bottom row, 'Stimulus' panel). These lines with negative slopes are created by the significant hold interval while the eyes are tracking the displayed moving object. Particularly, during each frame interval, the displayed stimulus remains stationary on our screen, while our eyes, however, are still following the global motion at a constant speed. As a result, the displayed stimulus appears to have a velocity opposite to the eye motion, leading to the negative-sloped line segments. The limited spatiotemporal bandwidth of our eyes, acting like a low-pass filter, blurs the individual lines and their boundaries become difficult to locate. Therefore, the envelope of the group of line segments is perceived as a single thick and blurry edge.

Since a longer hold interval expands the travel range of the displayed stimulus on our retina during each frame interval, motion blur will be exacerbated.

### C. Color breakup in field sequential RGB displays

In displays presenting colors sequentially, color breakup is another artifact that can disturb the viewing experience. Especially when viewers visually track the displayed stimulus, the breakup effect becomes exceedingly noticeable, at a significant hold interval (Fig. 7, middle row). As explained in the previous section, a long hold interval and object tracking can result in a blurred and expanded envelope of the original smooth motion trajectory. When the three colors are presented sequentially at even delays, each of the color will occupies one third of the entire displacement range of the displayed stimulus during each frame interval. As a result, the single chromatic white envelope is now divided into three monochromatic horizontal stripes, where the color presented first (red color in Fig. 7) has the minimum deviation from the continuous motion trajectory, and the color presented last (blue color in Fig. 7) locates furthest away. Since color breakup is an artifact resulted from

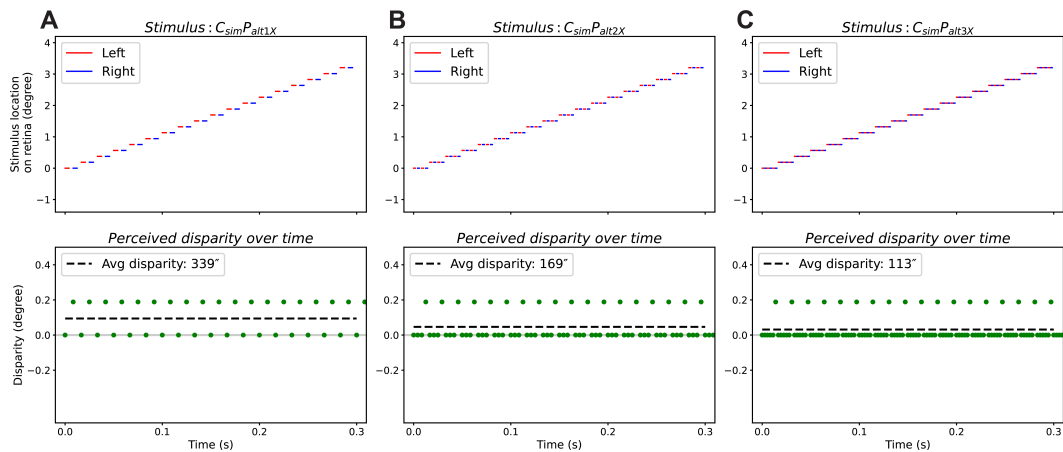


Fig. 8. Depth distortion suppressed with multi-flash protocol. Top row: stimulus presented to the viewers, where the same captured image of a moving object is presented alternatively to the left and right eyes during each frame. Bottom row: binocular disparity over time. (A - C) One sampled image is presented to each eye once, twice, and three times during each frame, respectively, where the average (perceived) disparity proportionally decreases with the number of flashes. Stimulus motion velocity:  $10\text{cm/s}$ . Frame rate:  $60\text{fps}$

varying displacements with respect to retina among colors, applying spatial offsets to compensate for the differences will extinguish this artifact [15]. The spatial offset required for each channel is:

$$\text{Offset}_i = (i - 1) \frac{vh}{3f} \quad (12)$$

where  $i$  is the presentation order for the color channel that is being corrected, ranging from 1 to 3,  $v$  is velocity of the stimulus,  $h$  is the hold interval, and  $f$  is the frame rate. Therefore, by adding spatial offsets to the green and blue colors in Fig. 7, the color breakup is successfully eliminated from the perceived stimulus (Fig. 7, bottom row).

#### D. Depth distortion in temporally interlacing stereoscopic displays

1) *Reducing depth distortion using multiple flashes:* Horizontally moving object can appear to be displaced in depth if the same image is sequentially presented to the two eyes for each frame. Within each frame interval, the two eyes are viewing the same stimulus, so the binocular disparity is 0. When the next image reflecting the new position of the object is presented to the preceding eye, however, a non-zero binocular disparity between the two eyes will occur. When the image is presented to the other eye, the disparity recovers to 0. Since the human visual system has no cue to decide which disparity is the correct, it will combine the two groups of disparities and output a depth cue using a time-weighted average [16]. Therefore, the object will appear displaced in depth. For example, in Fig. 8, the object is moving from left to right, and the order of image presentation to the eye is from left to right as well. As a result, the positive inter-frame disparity and average disparity creates an illusion to the viewer that the object is moving further away.

In contrast, if the same frame is presented more than once, i.e., the number of flashes is larger than 1, multiple 0 disparity values are detected during each frame interval, while the inter-frame disparity stays constant, leading to a smaller magnitude

of the mean disparity perceived by our visual system (Fig. 8A). The instantaneous inter-frame disparity is:

$$\text{Disparity} = \frac{v}{n_{\text{flash}} f} \quad (13)$$

The average disparity is calculated as:

$$\text{Disparity}_{\text{avg}} = \frac{v}{2n_{\text{flash}} f} \quad (14)$$

where  $n_{\text{flash}}$  is the number of flashes. As depicted in Fig. 8B,C, the average disparity was reduced by a factor of 2 and 3, when the number of flashes is 2 and 3, respectively.

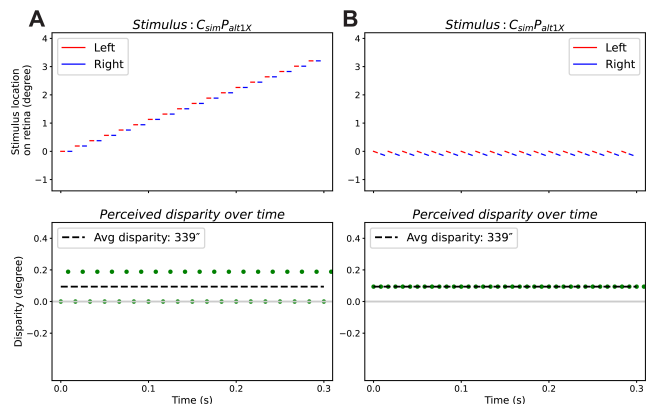


Fig. 9. Eye motion does not affect the perceived disparity. (A) Stimulus (top) and disparity (bottom) with eye fixation. (B) Stimulus (top) and disparity (bottom) with object tracking. Stimulus motion velocity (on display):  $10\text{cm/s}$ . Frame rate:  $60\text{fps}$

2) *The persistence of depth distortion with and without eye motion:* Despite the prevalence of object tracking and eye motion in the usage and applications of modern displays, to our knowledge, there is no quantification on depth distortion with eye motion in the context of temporally interlacing stereoscopic displays.

Using the average position of stimulus on the left and right retinas, the disparity within each frame and between two frames remains the same, so does the average disparity.

So the average disparity and instantaneous disparity are both expressed as:

$$Disparity = \frac{v}{2n_{flash}f} \quad (15)$$

Which is half the value defined by equation 13. An example comparison between the disparity with and without eye motion is displayed in Fig. 9. Without object tracking, the disparity oscillates between 0 and 678", while with object tracking, the disparity remains at half of the peak value, a constant 339". In both cases, the perceived average disparity is 339".

## V. CONCLUSIONS AND FUTURE DIRECTION

We developed a robust toolkit, BiPMAP, to predict and visualize the diverse variety of motion artifacts encountered when using modern displays. The toolkit accounts for a comprehensive list of user inputs, including the stimulus configuration, the viewing parameters and the display parameters. It enables effortless categorization of motion artifacts for any selected configuration via side-by-side comparisons of simulated perceived stimuli. With the comparison of continuous and sampled stimuli, one can easily simulate the elimination process of artifacts through the optimization of user inputs. Furthermore, although the standard frame rate in the television and film industry has remained the same for many years (60 Hz or 75 Hz [2]), we thoroughly demonstrated that the desired frame rate is highly dependent on the specific application. Therefore, many factors, such as the maximum velocity in the scene presented by the display, the luminance, and the occurrence of eye motion, need to be integrated during the design to ensure the best immersive experience. This toolkit, with an interactive user interface and robust computational model, made such integration possible. It has received broad interest from display manufacturers and is expected to play an important role in guiding the display design process.

So far, BiPMAP does not take into account any optical aberrations when predicting the perceived motion artifacts, while optical aberrations exist commonly in both XR headsets and human eyes. Adding a kernel preceding the CSF to represent any optical distortion to the presented stimuli will further improve the accuracy of our predictions. In addition, no eccentricity but only central vision is accounted for when the object is moving across the screen, and only 1D motion is modeled in this toolkit for computational simplicity. In the future, to address the needs for displays with a larger field of view, heterogeneous scenes, and 2D motion, a peripheral vision component can be incorporated into the model.

## REFERENCES

[1] A. Watson, A. Ahumada, and J. Farrell, "Window of visibility - a psychophysical theory of fidelity in time-sampled visual motion displays," *Journal of the Optical Society of America A*, vol. 3, 04 1986.

[2] A. Mackin, K. Noland, and D. Bull, "High frame rates and the visibility of motion artifacts," *SMPTE Motion Imaging Journal*, vol. 126, pp. 41–51, 07 2017.

[3] D. Hoffman, V. Karasev, and M. Banks, "Temporal presentation protocols in stereoscopic displays: Flicker visibility, perceived motion, and perceived depth," *Journal of the Society for Information Display*, vol. 19, pp. 271–297, 03 2011.

[4] A. B. Watson, "High frame rates and human vision: A view through the window of visibility," *SMPTE Motion Imaging Journal*, vol. 122, no. 2, pp. 18–32, 2013.

[5] P. Johnson, J. Kim, D. Hoffman, A. Vargas, and M. Banks, "Motion artifacts on 240-hz oled stereoscopic 3d displays: Motion artifacts on 240-hz oled s3d displays," *Journal of the Society for Information Display*, vol. 22, 02 2015.

[6] S. Daly, N. Xu, J. Crenshaw, and V. Zunjarrao, "A psychophysical study exploring judder using fundamental signals and complex imagery," vol. 124, 10 2014.

[7] A. Watson and A. Ahumada, "The pyramid of visibility," in *Electronic Imaging 16*, 01 2016, pp. 37–42.

[8] R. Mantiuk, M. Ashraf, and A. Chapiro, "stelacsf: a unified model of contrast sensitivity as the function of spatio-temporal frequency, eccentricity, luminance and area," *ACM Transactions on Graphics*, vol. 41, pp. 1–16, 07 2022.

[9] A. Watson, "The field of view, the field of resolution, and the field of contrast sensitivity," *Journal of Perceptual Imaging*, 01 2018.

[10] P. G. J. Barten, "Formula for the contrast sensitivity of the human eye," in *Image Quality and System Performance*, vol. 5294, International Society for Optics and Photonics. SPIE, 2003, pp. 231–238.

[11] M. Mori, T. Hatada, K. Ishikawa, T. Saishouji, O. Wada, J. Nakamura, and N. Terashima, "Mechanism of color breakup on field-sequential color projectors," *SID Symposium Digest of Technical Papers*, vol. 30, no. 1, pp. 350–353, 1999.

[12] C.-H. Chen, F.-C. Lin, Y.-T. Hsu, Y.-P. Huang, and H.-P. Shieh, "A field sequential color lcd based on color fields arrangement for color breakup and flicker reduction," *Journal of Display Technology*, vol. 5, pp. 34–39, 01 2009.

[13] F.-C. Lin, Y.-P. Huang, and H.-P. D. Shieh, "Color breakup reduction by 180 hz stencil-fsc method in large-sized color filter-less lcds," *J. Display Technol.*, vol. 6, no. 3, pp. 107–112, Mar 2010.

[14] Z. Qin, Y. Zhang, F.-C. Lin, Y.-P. Huang, and H. Shieh, "A review of color breakup assessment for field sequential color display," *Information Display*, vol. 35, pp. 13–43, 04 2019.

[15] P. Johnson, J. Kim, and M. Banks, "The visibility of color breakup and a means to reduce it," *Journal of vision*, vol. 14, 12 2014.

[16] M. S. Banks, D. M. Hoffman, J. Kim, and G. Wetzstein, "3d displays," *Annual Review of Vision Science*, vol. 2, no. 1, pp. 397–435, 2016, PMID: 28532351.

[17] M. Morgan, "Perception of continuity in stroboscopic motion: A temporal frequency analysis," *Vision Research*, vol. 19, no. 5, pp. 491–500, 1979.

[18] D. C. Burr and J. Ross, "How does binocular delay give information about depth?" *Vision Research*, vol. 19, pp. 523–532, 1979.

[19] A. Watson, "Temporal sensitivity," in *Handbook of Perception and Human Performance*. Wiley, 1986, ch. 6.

[20] H. de Lange, "Research into the dynamic nature of the human fovea→cortex systems with intermittent and modulated light. i. attenuation characteristics with white and colored light," *J. Opt. Soc. Am.*, vol. 48, no. 11, pp. 777–784, Nov 1958.